Research Journal of
Phytochemistry

ISSN 1819-3471

Academic
Journals Inc.

www.academicjournals.com

Research Journal of Phytochemistry 9 (4): 144-160, 2015
ISSN 1819-3471 / DOI: 10.3923/rjphyto.2015.144.160

Phytochemical Synthesis and Crystallization of Sucrose from the Extract of *Gloriosa superba*

[1]K. Gopinath, [2]C. Karthikeyan, [2]A.S. Haja Hameed, [3]K. Arunkumar and [1]A. Arumugam
[1]Department of Nanoscience and Technology, Alagappa University, Karaikudi, 630003, Tamil Nadu, India
[2]PG and Research Department of Physics, Jamal Mohamed College, Tiruchirappalli, 620020, Tamil Nadu, India
[3]PG and Research Department of Botany, Alagappa Government Arts and Science Collage, Alagappa Univesity, Karakudi, 630003, Tamil Nadu, India

Corresponding Author: A. Arumugam, Department of Nanoscience and Technology, Alagappa University, Karaikudi, 630003, Tamil Nadu, India Tel: +91 4565 225630 Fax: +91 4565 225202

ABSTRACT

Sucrose is a major commodity in worldwide. In half a century the progress towards the understanding of the chemistry, structure, physical and functional properties of the sucrose molecule have been rapid. It was crystallized from the hot methanol extract of the rhizome powder of *Gloriosa superba* by using slow evaporation method at room temperature. The synthesized sucrose crystal lattice parameters were characterized by single crystal X-ray diffraction analysis. The presences of organic functional groups in the grown crystal were identified by FT-IR and Micro Raman analyses. The optical parameter of the grown single crystal was analyzed by UV-visible spectroscopy and maximum absorption was occurred at 253 nm. In addition, HOMO, LUMO, Molecular Electrostatic Potential (MESP), non-linear optical and several thermodynamic properties were analyzed by the DFT calculations. The thermal degradation of the sucrose crystal was tested by Thermo Gravimetric/Differential Thermal Analysis (TG/DTA).

Key words: Single crystal X-ray diffraction, FT-IR, Micro Raman, HOMO-LUMO, DFT

INTRODUCTION

Sucrose ($C_{12}H_{22}O_{11}$) is an organic compound, a nonreducing disaccharide composed of glucose and fructose linked their anomeric carbons. The molecular structure of sucrose ((2-[3,4-dihydroxy-2,5-bis(hydroxymethyl) oxolan-2-yl] oxy-6-(hydroxymethyl) oxane-3,4,5-triol) has been determined by X-ray reflections (Hynes and Page, 1991; Hanson *et al*., 1973). It was widely distributed and has been found universally throughout the plant kingdom in fruits, seeds, flowers, roots and tubers. It is obtained commercially from sugarcane (*Saccharum officinarum*), sugar beet (*Beta vulgaris*), palm (*Borassus flabellifer*) and soyben (*Glycine max*) (Kumaresan and Babu, 1997; Kraybill *et al*., 1937). Sucrose is widely used in food industry, bakery products and act to inhibit the growth of microorganisms due to the higher concentration gradient of sucrose molecule. For long periods, a considerable number of experimental studies related to sucrose have been published due to the physical and chemical properties. Recently, sucrose is used as a promising material for dosimetry (Nakajima and Otsuki, 1990; Hamzaoui *et al*., 2009; Peimel-Stuglik, 2010), hologram (Ponce-Lee *et al*., 2004), biological probe (Predoi, 2010), X-ray osteodensitometry (Ryzhikov *et al*., 2005), nonlinear optics (Kaminskii, 2003), phase transition (Son *et al*., 2010), Low-temperature electrolytic coloration (Gu *et al*., 2012) and cryoprotectant (Luzardo *et al*., 2000).

Gloriosa superba L., (Colchicaceae) is a greenish, climbing herb. It is native of South Africa. It is a national flower of Zimbabwe and state flower of Tamil Nadu. *Gloriosa superba* is a tuberous plant with plow shaped cylindrical tubers. It is commercially cultivated in Tamil Nadu and particularly in Karur and Moolanur region. It has been used for arthritis, gout, rheumatism, inflammation, ulcers, bleeding piles, skin diseases, leprosy and snakebites (Kumar *et al*., 2015; Arumugam *et al*., 2015; Chitra and Rajamani, 2010; Jana and Shekhawat, 2011). The tubers and seeds of this plant contain two major alkaloids namely colchicines and colchicosides. Colchicines were used for anti-cancer drug and plant breeding research (Arumugam and Gopinath, 2012; Ramalakshmi *et al*., 2012; Bharathi *et al*., 2006; Yadava *et al*., 2013).

We have successfully isolated the sucrose crystal derived from the hot methanol (MeOH) extract of the rhizome powder of *G. superba*. The grown crystal has been characterized with single crystal X-ray diffraction, FT-IR, Micro Raman, UV-visible spectroscopy and TG-DTA analyses. Using density functional theory, HOMO-LUMO, Molecular Electrostatic Potential (MEP), first order hyperpolarizability and thermodyanmic properties are analyzed using B3LYP/6-311 G(d, p) basis sets for the sucrose molecule. To our knowledge, this is the first report for the phytosynthesis of new sucrose crystal derived from the rhizome of *G. superba*.

MATERIALS AND METHODS

Plant collection and extraction: *Gloriosa superba* rhizomes were collected from Glorious Endangered Medicinal Plants Conservation Centre, Science Campus, Alagappa University, Karaikudi, Tamil Nadu, India. The taxonomic identification was made by Dr. S. John Britto, The Rapinat Herbarium and Centre for Molecular Systematics, St. Joseph's College (Campus), Tiruchirappalli, Tamil Nadu, India. The voucher specimen was numbered (KG-001) and herbarium kept in our Department of Nanoscience and Technology. The collected *G. superba* rhizomes were cleaned with tap water to remove the soil particles, then samples cut into pieces of 0.5-1.0 cm. All the samples were dried in shadow for one week and grind to fine powder. The 20 g of powders were extracted with 350 mL of MeOH in a soxhlet extractor for 6 h. The extract in yellow color was changed to reddish wine color after the continuous extraction. The excess solvent was evaporated with the rotary evaporator. Finally, 50 mL of solvent mixed compounds were filtered through Whatman No. 1 filter paper and stored at vials. Sucrose crystals successfully grew on the sides of the flask by the slow evaporation method at room temperature.

Characterization: Single crystal X-ray intensity data of sucrose was collected at room temperature (T = 296 K) on a Bruker X8 KAPPA APEX-II CCD diffractometer equipped with graphite monochromated Mo Kα radiation. Initial unit cell parameters were obtained from SMART V5.05 software for CCD detector system; Bruker Analytical X-ray Systems, Madison, WI, 1998. Data integration, correction for Lorentz polarization effects and final cell refinement were performed by SAINTPLUS, V5.00 Software for the CCD detector system; Bruker Analytical X-Ray System, Inc.: Madison, WI, 1998. An empirical absorption correction based on the multiple measurements of equivalent reflections was applied using SADABS, Program for absorption correction using SMART CCD based on the method of Blessing (1995). Structure was obtained by a combination of the direct methods and difference Fourier syntheses and refined by full-matrix least-squares on F^2 using the SHELXTL (Thamilarasan *et al*., 2013). All non hydrogen atoms were

refined anisotropically. All hydrogen atoms were replaced in ideal positions and refined as riding atoms with relative isotropic displacement parameters. Liquid state ^{1}H and ^{13}C NMR spectra were recorded on a BRUKER 400 MHz spectrometer. The proton spectra at 400 MHz were recorded at room temperature (33.2°C). Samples were prepared by dissolving about 0.25 g of the sample in 2.5 mL of DMSO. Proton spectrum has the following experimental parameters. Number of scans 15, spectral width 10000.00 Hz, acquisition time 1.63 sec. The carbon (^{13}C) NMR spectra at 100 MHz were recorded at room temperature on the same instrument. The samples were prepared by dissolving about 0.25 g of the sample in 2.5 mL of DMSO. Proton spectrum following experimental parameter: Number of scan 587, spectral width 29761.904 Mz, acquisition time 0.55 sec. Fourier transform infrared spectroscopy (FT-IR) measurements were prepared by sucrose powder with KBr. This powder was then compressed into a thin pellet consist of 12 mm in diameter and about 15 mg in weight. Spectrum was recorded in the 4000-400 cm^{-1} region. The Micro Raman analysis of our sample was carried out in the instrument of Princeton Acton SP2500, Cs spectrometer 0.5 focal length triple grating monochromator excitation source, Ar^{+} Laser, 514.5 nm wavelength. The UV-visible spectrum of the sucrose was obtained for the wavelength in the range of 200-900 nm using Shimadzu spectrophotometer (Model UV-1800) operating at a resolution of 1 nm. The Density Functional Theory (DFT) was used for HOMO-LUMO analysis, Molecular Electrostatic Potential (MESP), first order hyperpolarizability and thermodynamic properties by means of the hybrid functional DFT/B3LYP with the 6-311 G(d, p) basis set available in Gaussian 09 Program (Casado *et al*., 2002; Lee *et al*., 1988). The thermal behavior of the sucrose crystals was studied with TGA and DTA in a nitrogen atmosphere, using 'Seiko SSC 5200 H' model analyzer.

RESULTS AND DISCUSSION

Single crystal X-ray diffraction: The crystal obtained by slow evaporation method crystal was subjected to single crystal X-ray diffraction (Fig. 1a-b) and it structure was solved and refined. Table 1-2 show the detailed report of the structure refinement and hydrogen coordinates of crystal. Sucrose crystals are monoclinic space group as P21 with unit cell dimensions of a = 7.7540 Å, b = 8.7130 Å, c = 10. 8600Å and β = 103.0380. The ORTEP diagram is shown in Fig. 2. The atomic displacement parameters ($Å^2$) are given in Table 3. Sucrose crystal structures consists of two rings which namely glucopyran ring and glucofuran ring. The glucopyran ring C5-O4-C4 and glucofuran ring C7-O8-C10 the bond angles of 115.82 and 111.69°. The inter connection of oxygen molecule binding with glucopyran ring and glucofuran ring C5-O6-C7 bond length are 113.72°. The bond length, bond angle and torsion angles are given in Table 4. The hydrogen bonds of the sucrose crystal are O-H…O highest>DHA values attributed to the O1-H (1A)…O9 for 174° and hydrogen bonds are given in Table 5. The molecular packing of sucrose crystal along of a-axis, b-axis and c-axis is shown in Fig. 3.

^{1}H, ^{13}C, NMR, DMSO-D6-300 MHz: ^{1}H NMR (Fig. 4) 3.138-3.107 (m, 2 H), 3.181-3.155 (m, 2 H), 3.396 (s, 2 H), 3.560 (s, 4 H), 3.643 (m, 1 H) 3.767 (Q, J = 15 Hz, 1 H), 3.758 (d, J = 9.9 Hz, 1 H) 4.372 (d, J = 4.5 Hz, 2 H) 4.501 (d, J = 6 Hz, 1 H) 4.797 (t, J = 8.7 Hz, 3 H), 5.7173 (s, 1 H), 5.184 (s1, 2 H). ^{13}C NMR (Fig. 5) C1-62.57, C2-70.27, C3-72.07 C4-73.26, C5-74.70, C6-77.43, C7-83.00, C8-92.18, C9-104.17.

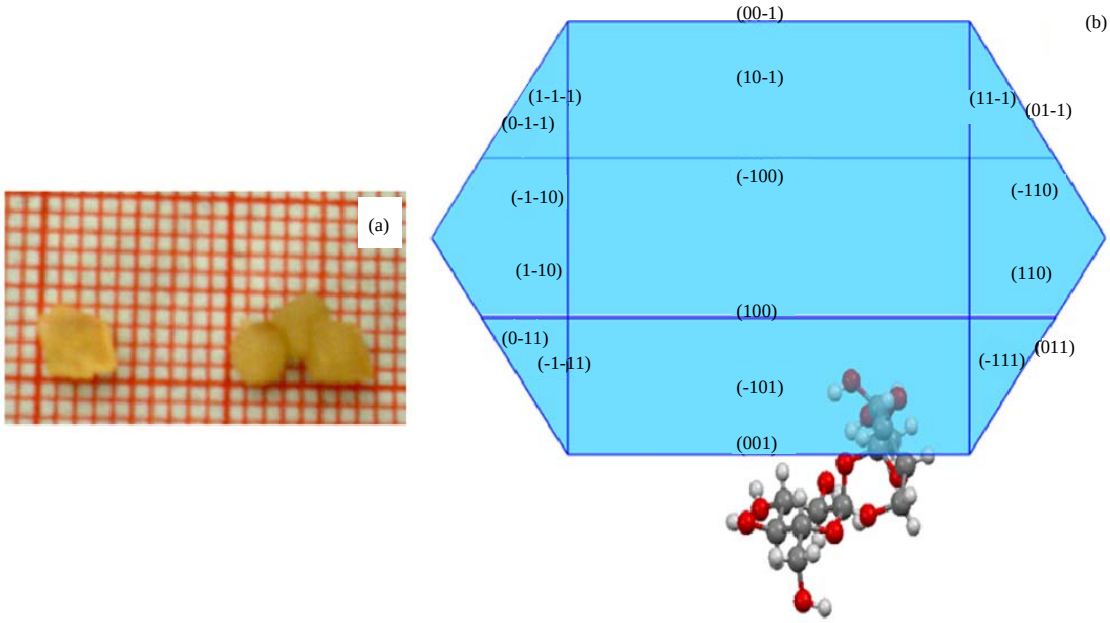

Fig. 1(a-b): (a) Photograph of sucrose single crystal and (b) Schematic of sucrose crystal using (Mercury 2.4 software)

Table 1: Single crystal X-ray diffraction data of sucrose crystal

Identification code	Sucrose crystal
Empirical formula	C_{12} H_{22} O_{11}
Formula weight	342.30
Temperature	293 (2) K
Wavelength	0.71073 Å
Crystal system	Monoclinic
Space group	P21
Unit cell dimensions	
a (Å)	7.7540 (2)
b (Å)	8.7130 (2)
c (Å)	10.86000 (10)
α (°)	90
β (°)	103.0380 (10)
γ (°)	90
Volume	714.79 (3) $Å^3$
Z, Calculated density	2, 1.590 Mg m^{-3}
Absorption coefficient	0.142 mm^{-1}
F(000)	364
Crystal size	0.35×0.30×0.20 mm
Theta range for data collection	2.70 to 24.99 deg.
Limiting indices	-7<=h<=9, -10<=k<=10, -12<=l<=12
Reflections collected/unique	6820/2450 [R(int) = 0.0249]
Completeness to theta	= 24.99 99.9%
Absorption correction	Semi-empirical from equivalents
Max. and min. transmission	0.9865 and 0.9145
Refinement method	Full-matrix least-squares on F^2
Data/restraints/parameters	2450/1/240
Goodness-of-fit on F^2	1.077
Final R indices [I>2sigma(I)]	R1 = 0.0229, wR2 = 0.0589
R indices (all data)	R1 = 0.0235, wR2 = 0.0593
Absolute structure parameter	-0.1(7)
Largest diff. peak and hole	0.163 and -0.155 e.$Å^3$

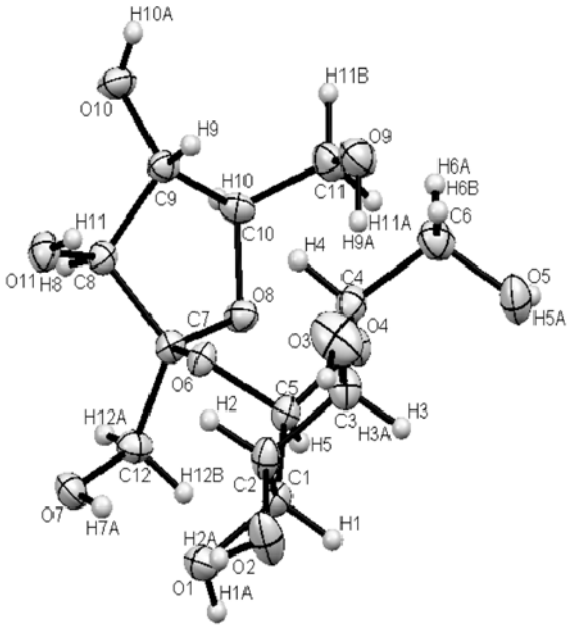

Fig. 2: ORTEP diagram of sucrose crystal

Table 2: Hydrogen coordinates ($\times 10^4$) and isotropic displacement parameters ($Å^2 \times 10^3$)

Atom	X	Y	Z	U(eq)
C (1)	6355 (2)	2343 (2)	8127 (1)	23 (1)
C (2)	5642 (2)	728 (2)	7857 (1)	25 (1)
C (3)	4421 (2)	382 (2)	8739 (2)	26 (1)
C (4)	2955 (2)	1572 (2)	8591 (1)	25 (1)
C (5)	4854 (2)	3513 (2)	8001 (1)	20 (1)
C (6)	1840 (2)	1383 (2)	9569 (2)	31 (1)
C (7)	3698 (2)	5165 (2)	6246 (1)	20 (1)
C (8)	2146 (2)	5184 (2)	5073 (1)	20 (1)
C (9)	554 (2)	5421 (2)	5651 (1)	22 (1)
C (10)	1285 (2)	6476 (2)	6763 (1)	23 (1)
C (11)	471 (2)	6272 (2)	7890 (2)	30 (1)
C (12)	5434 (2)	5782 (2)	6032 (2)	25 (1)
O (1)	7473 (2)	2731 (2)	7290 (1)	29 (1)
O (2)	7027 (2)	-387 (2)	8090 (1)	39 (1)
O (3)	3554 (2)	-1047 (2)	8486 (2)	46 (1)
O (4)	3686 (1)	3104 (1)	8774 (1)	23 (1)
O (5)	2859 (2)	1634 (2)	10816 (1)	36 (1)
O (6)	3911 (1)	3623 (1)	6713 (1)	19 (1)
O (7)	6208 (1)	4737 (2)	5299 (1)	30 (1)
O (8)	3163 (1)	6146 (1)	7122 (1)	23 (1)
O (9)	398 (2)	4709 (2)	8268 (1)	35 (1)
O (10)	-894 (2)	6118 (2)	4783 (1)	30 (1)
O (11)	2042 (1)	3913 (2)	4259 (1)	27 (1)

FT-IR and Micro-Raman spectroscopy: The sucrose sample is characterized by FT-IR and Micro-Raman spectra in order to identify the functional groups and detect the vibration modes of molecules of the sample shown in Fig. 6a-b. Generally the hydroxyl groups are observed in around 3500-3600 cm^{-1} (Michalska *et al*., 1996). The O-H group vibrations are likely to be the most sensitive to the environment, so they show pronounced shift in the spectra of hydrogen bond species. The band due to the O-H stretching appears at 3335 cm^{-1} in IR spectrum and strong

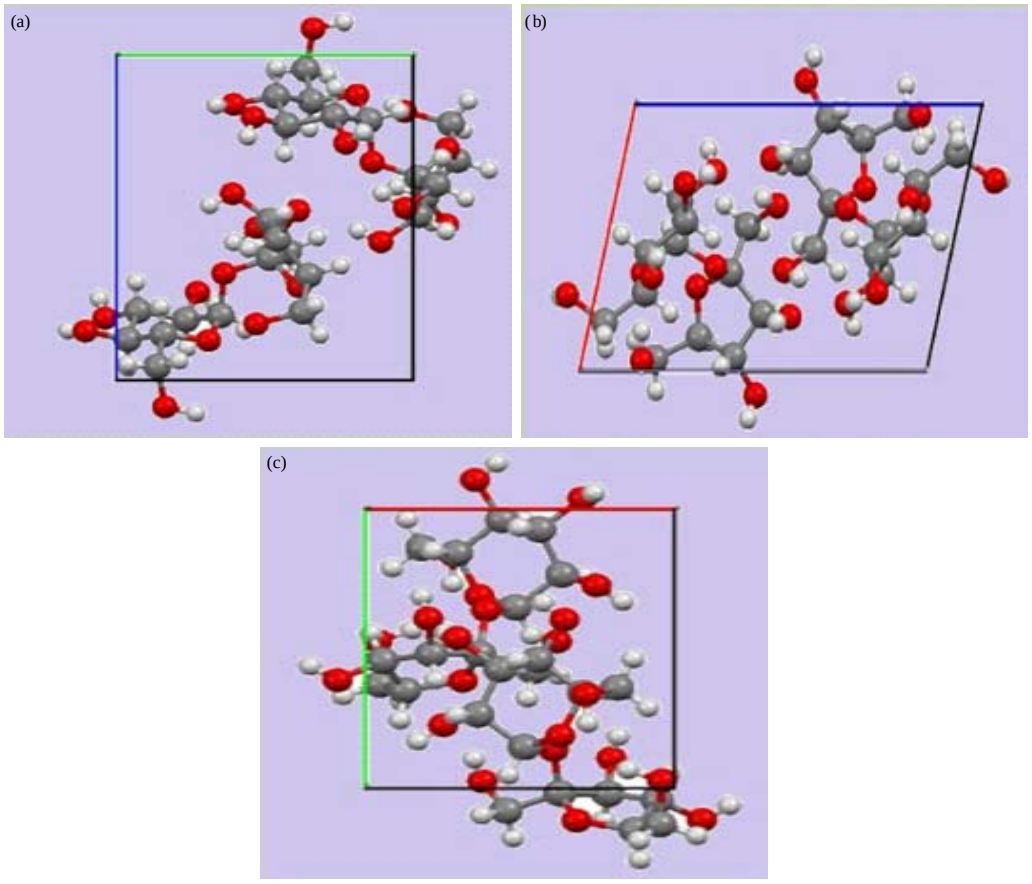

Fig. 3(a-c): Molecular packing of sucrose crystal packing along (a) b axis (b) a axis and (c) c axis diagram

Table 3: Atomic displacement parameters (Å^2)

Atom	U11	U22	U33	U23	U13	U12
C (1)	22 (1)	27 (1)	18 (1)	2 (1)	2 (1)	2 (1)
C (2)	33 (1)	23 (1)	19 (1)	2 (1)	5 (1)	5 (1)
C (3)	34 (1)	21 (1)	24 (1)	0 (1)	8 (1)	-2 (1)
C (4)	27 (1)	25 (1)	22 (1)	2 (1)	4 (1)	-4 (1)
C (5)	22 (1)	20 (1)	17 (1)	-1 (1)	3 (1)	0 (1)
C (6)	31 (1)	32 (1)	33 (1)	6 (1)	11 (1)	0 (1)
C (7)	20 (1)	17 (1)	21 (1)	0 (1)	4 (1)	0 (1)
C (8)	20 (1)	20 (1)	20 (1)	2 (1)	3 (1)	-2 (1)
C (9)	18 (1)	23 (1)	23 (1)	5 (1)	3 (1)	1 (1)
C (10)	19 (1)	21 (1)	30 (1)	0 (1)	6 (1)	3 (1)
C (11)	28 (1)	35 (1)	31 (1)	-5 (1)	11 (1)	2 (1)
C (12)	20 (1)	25 (1)	30 (1)	2 (1)	6 (1)	-2 (1)
O (1)	22 (1)	34 (1)	31 (1)	2 (1)	8 (1)	1 (1)
O (2)	54 (1)	31 (1)	36 (1)	10 (1)	22 (1)	20 (1)
O (3)	51 (1)	23 (1)	68 (1)	-7 (1)	25 (1)	-8 (1)
O (4)	27 (1)	22 (1)	21 (1)	-1 (1)	9 (1)	0 (1)
O (5)	47 (1)	38 (1)	26 (1)	5 (1)	14 (1)	7 (1)
O (6)	22 (1)	17 (1)	17 (1)	1 (1)	2 (1)	-1 (1)
O (7)	26 (1)	38 (1)	30 (1)	4 (1)	13 (1)	1 (1)
O (8)	19 (1)	25 (1)	25 (1)	-7 (1)	3 (1)	1 (1)
O (9)	29 (1)	42 (1)	36 (1)	8 (1)	12 (1)	2 (1)
O (10)	18 (1)	39 (1)	32 (1)	8 (1)	1 (1)	3 (1)
O (11)	30 (1)	27 (1)	22 (1)	-4 (1)	5 (1)	-3 (1)

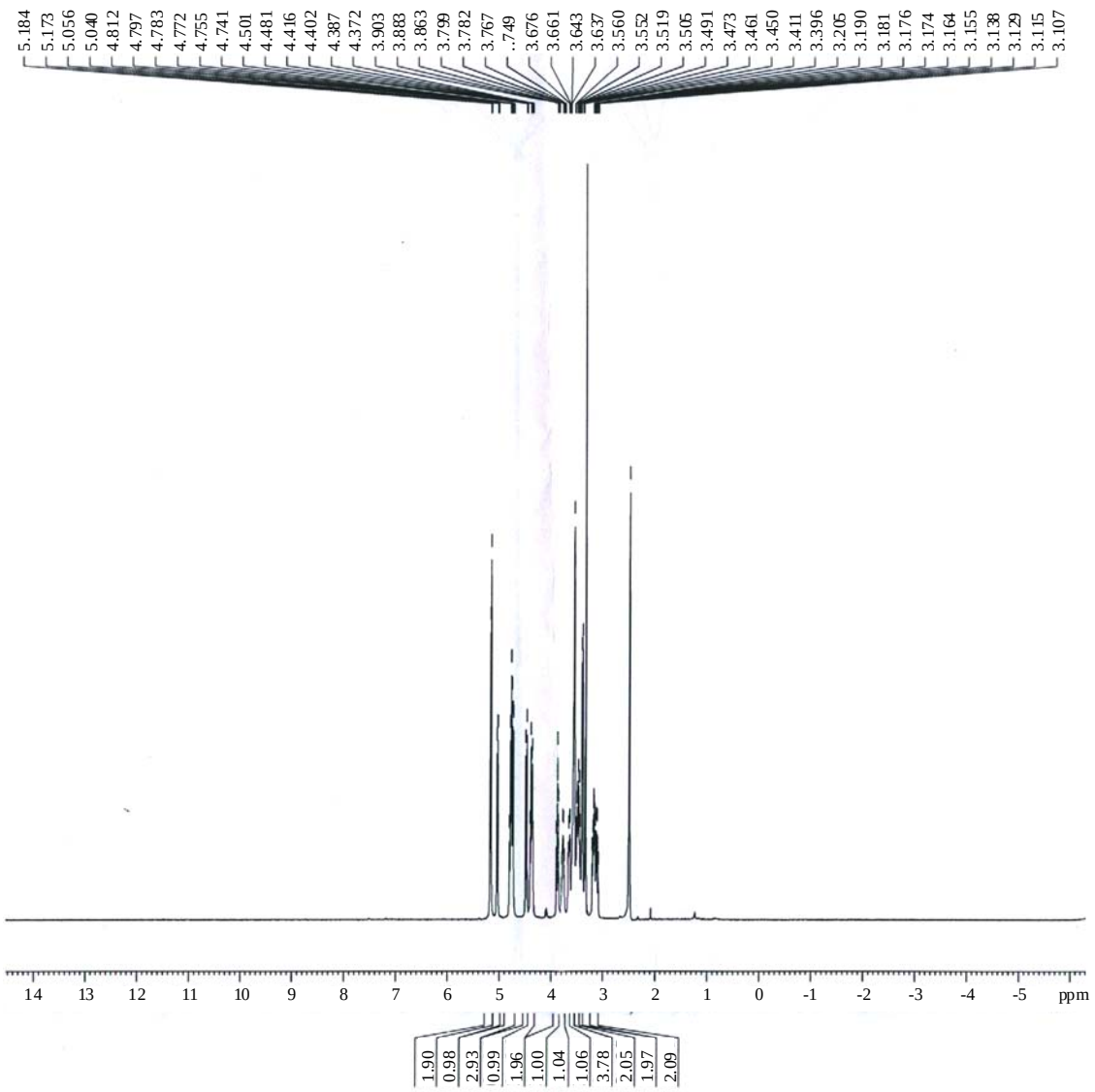

Fig. 4: ^{1}H-NMR analysis of sucrose crystal

band appears in 3227 cm^{-1} from Raman spectrum. The FT-IR band observed at 2923 cm^{-1} have been assigned to CH_2 symmetric stretching vibrations. The CH_2bending modes follow in decreasing frequency, the general order CH_2 deformation>CH_2 Scis>CH_2 Wagg>CH_2 twist>CH_2 rock>. Since the bending modes involving the hydrogen atom attached to the central carbon atoms falls in 1440-1312 cm^{-1} range, there is extensive vibrational coupling of these modes with CH_2 twist. It is not that ρ $CH_2$and r CH_2 are sensitive to the molecular conformation. The scissoring modes can be assigned to the medium IR and Raman bands at 1356 and 1312 cm^{-1}. The out-of-plane deformation modes (τOH and γOH) observed values are 1239 and 1248 cm^{-1} from IR and Raman spectrum. The IR bands are observed at 1067 cm^{-1} owing to the stretching of C-O-C in sucrose (Jantas and Delczyk, 2005; Naumann *et al*., 1996). The C-C stretching modes are strongly coupled with other modes at 676, 917 and 1192 cm^{-1} from IR spectrum. The glucofuran ring deformation is clearly assigned to the IR band at 558 cm^{-1}.

Table 4: Bond length (Å), bond angles (°) and torsion angles (°) of sucrose crystals

Bond length	Values (Å)	Bond angles	Values (°)	Torsion angles	Values (°)
C (1)-O (1)	1.4316 (19)	O (1)-C (1)-C (2)	110.06 (13)	O (1)-C (1)-C (2)-O (2)	63.20 (15)
C (1)-C (2)	1.516 (2)	O (1)-C (1)-C (5)	110.08 (12)	C (5)-C (1)-C (2)-O (2)	-174.41 (12)
C (1)-C (5)	1.530 (2)	C (2)-C (1)-C (5)	111.38 (12)	O (1)-C (1)-C (2)-C (3)	-178.34 (12)
C (1)-H (1)	0.98	O (1)-C (1)-H (1)	108.4	C (5)-C (1)-C (2)-C (3)	-55.95 (15)
C (2)-O (2)	1.427 (2)	C (2)-C (1)-H (1)	108.4	O (2)-C (2)-C (3)-O (3)	-64.55 (18)
C (2)-C (3)	1.521 (2)	C (5)-C (1)-H (1)	108.4	C (1)-C (2)-C (3)-O (3)	174.46 (14)
C (2)-H (2)	0.98	O (2)-C (2)-C (1)	111.74 (13)	O (2)-C (2)-C (3)-C (4)	177.26 (13)
C (3)-O (3)	1.412 (2)	O (2)-C (2)-C (3)	107.72 (13)	C (1)-C (2)-C (3)-C (4)	56.28 (16)
C (3)-C (4)	1.521 (2)	C (1)-C (2)-C (3)	108.26 (13)	O (3)-C (3)-C (4)-O (4)	-177.41 (12)
C (3)-H (3)	0.98	O (2)-C (2)-H (2)	109.7	C (2)-C (3)-C (4)-O (4)	-54.89 (16)
C (4)-O (4)	1.446 (2)	C (1)-C (2)-H (2)	109.7	O (3)-C (3)-C (4)-C (6)	64.54 (17)
C (4)-C (6)	1.522 (2)	C (3)-C (2)-H (2)	109.7	C (2)-C (3)-C (4)-C (6)	-172.93 (13)
C (4)-H (4)	0.98	O (3)-C (3)-C (4)	105.59 (14)	O (1)-C (1)-C (5)-O (4)	177.03 (11)
C (5)-O (4)	1.4119 (18)	O (3)-C (3)-C (2)	112.87 (14)	C (2)-C (1)-C (5)-O (4)	54.65 (16)
C (5)-O (6)	1.4283 (17)	C (4)-C (3)-C (2)	110.81 (13)	O (1)-C (1)-C (5)-O (6)	54.96 (16)
C (5)-H (5)	0.98	O (3)-C (3)-H (3)	109.2	C (2)-C (1)-C (5)-O (6)	-67.41 (15)
C (6)-O (5)	1.423 (2)	C (4)-C (3)-H (3)	109.2	O (4)-C (4)-C (6)-O (5)	-56.95 (17)
C (6)-H (6A)	0.97	C (2)-C (3)-H (3)	109.2	C (3)-C (4)-C (6)-O (5)	64.00 (19)
C (6)-H (6B)	0.97	O (4)-C (4)-C (3)	110.73 (12)	O (8)-C (7)-C (8)-O (11)	-157.67 (12)
C (7)-O (8)	1.4088 (18)	O (4)-C (4)-C (6)	105.75 (13)	O (6)-C (7)-C (8)-O (11)	-39.21 (16)
C (7)-O (6)	1.4328 (18)	C (3)-C (4)-C (6)	112.43 (13)	C (12)-C (7)-C (8)-O (11)	84.81 (16)
C (7)-C (12)	1.5158 (19)	O (4)-C (4)-H (4)	109.3	O (8)-C (7)-C (8)-C (9)	-31.27 (15)
C (7)-C (8)	1.5430 (19)	C (3)-C (4)-H (4)	109.3	O (6)-C (7)-C (8)-C (9)	87.20 (13)
C (8)-O (11)	1.4076 (18)	C (6)-C (4)-H (4)	109.3	C (12)-C (7)-C (8)-C (9)	-148.79 (13)
C (8)-C (9)	1.520 (2)	O (4)-C (5)-O (6)	110.11 (11)	O (11)-C (8)-C (9)-O (10)	-78.57 (17)
C (8)-H (8)	0.98	O (4)-C (5)-C (1)	110.85 (12)	C (7)-C (8)-C (9)-O (10)	154.86 (12)
C (9)-O (10)	1.4285 (18)	O (6)-C (5)-C (1)	110.07 (11)	O (11)-C (8)-C (9)-C (10)	161.93 (12)
C (9)-C (10)	1.522 (2)	O (4)-C (5)-H (5)	108.6	C (7)-C (8)-C (9)-C (10)	35.36 (15)
C (9)-H (9)	0.98	O (6)-C (5)-H (5)	108.6	O (10)-C (9)-C (10)-O (8)	-147.54 (12)
C (10)-O (8)	1.4493 (17)	C (1)-C (5)-H (5)	108.6	C (8)-C (9)-C (10)-O (8)	-27.52 (15)
C (10)-C (11)	1.509 (2)	O (5)-C (6)-C (4)	111.50 (13)	O (10)-C (9)-C (10)-C (11)	91.44 (16)
C (10)-H (10)	0.98	O (5)-C (6)-H (6A)	109.3	C (8)-C (9)-C (10)-C (11)	-148.54 (13)
C (11)-O (9)	1.427 (2)	C (4)-C (6)-H (6A)	109.3	O (8)-C (10)-C (11)-O (9)	-69.86 (17)
C (11)-H (11A)	0.97	O (5)-C (6)-H (6B)	109.3	C (9)-C (10)-C (11)-O (9)	48.75 (19)
C (11)-H (11B)	0.97	C (4)-C (6)-H (6B)	109.3	O (8)-C (7)-C (12)-O (7)	171.55 (12)
C (12)-O (7)	1.428 (2)	H (6A)-C (6)-H (6B)	108	O (6)-C (7)-C (12)-O (7)	50.46 (16)
C (12)-H (12A)	0.97	O (8)-C (7)-O (6)	111.01 (11)	C (8)-C (7)-C (12)-O (7)	-72.19 (16)
C (12)-H (12B)	0.97	O (8)-C (7)-C (12)	107.16 (12)	O (6)-C (5)-O (4)-C (4)	67.72 (15)
O (1)-H (1A)	0.83 (3)	O (6)-C (7)-C (12)	110.55 (12)	C (1)-C (5)-O (4)-C (4)	-54.32 (15)
O (2)-H (2A)	0.77 (2)	O (8)-C (7)-C (8)	104.94 (11)	C (3)-C (4)-O (4)-C (5)	54.90 (15)
O (3)-H (3A)	0.76 (3)	O (6)-C (7)-C (8)	107.98 (11)	C (6)-C (4)-O (4)-C (5)	176.94 (11)
O (5)-H (5A)	0.92 (3)	C (12)-C (7)-C (8)	115.08 (12)	O (4)-C (5)-O (6)-C (7)	108.30 (13)
O (7)-H (7A)	0.85 (3)	O (11)-C (8)-C (9)	115.42 (12)	C (1)-C (5)-O (6)-C (7)	-129.20 (12)
O (9)-H (9A)	0.90 (3)	O (11)-C (8)-C (7)	115.68 (12)	O (8)-C (7)-O (6)-C (5)	-45.29 (15)
O (10)-H (10A)	0.84 (2)	C (9)-C (8)-C (7)	102.40 (11)	C (12)-C (7)-O (6)-C (5)	73.49 (14)
O (11)-H (11)	0.81 (3)	O (11)-C (8)-H (8)	107.6	C (8)-C (7)-O (6)-C (5)	-159.80 (11)
		C (9)-C (8)-H (8)	107.6	O (6)-C (7)-O (8)-C (10)	-101.80 (13)
		C (7)-C (8)-H (8)	107.6	C (12)-C (7)-O (8)-C (10)	137.39 (12)
		O (10)-C (9)-C (8)	112.06 (12)	C (8)-C (7)-O (8)-C (10)	14.60 (15)
		O (10)-C (9)-C (10)	111.30 (13)	C (11)-C (10)-O (8)-C (7)	132.59 (13)
		C (8)-C (9)-C (10)	102.62 (11)	C (9)-C (10)-O (8)-C (7)	8.15 (16)
		O (10)-C (9)-H (9)	110.2		
		C (8)-C (9)-H (9)	110.2		
		C (10)-C (9)-H (9)	110.2		
		O (8)-C (10)-C (11)	109.74 (12)		
		O (8)-C (10)-C (9)	105.38 (11)		
		C (11)-C (10)-C (9)	115.07 (13)		
		O (8)-C (10)-H (10)	108.8		
		C (11)-C (10)-H (10)	108.8		
		C (9)-C (10)-H (10)	108.8		
		O (9)-C (11)-C (10)	113.35 (13)		

Table 4: Continue

Bond length	Values (Å)	Bond angles	Values (°)	Torsion angles	Values (°)
		O (9)-C (11)-H (11A)	108.9		
		C (10)-C (11)-H (11A)	108.9		
		O (9)-C (11)-H (11B)	108.9		
		C (10)-C (11)-H (11B)	108.9		
		H (11A)-C (11)-H (11B)	107.7		
		O (7)-C (12)-C (7)	111.02 (13)		
		O (7)-C (12)-H (12A)	109.4		
		C (7)-C (12)-H (12A)	109.4		
		O (7)-C (12)-H (12B)	109.4		
		C (7)-C (12)-H (12B)	109.4		
		H (12A)-C (12)-H (12B)	108		
		C (1)-O (1)-H (1A)	112.7 (17)		
		C (2)-O (2)-H (2A)	113.8 (17)		
		C (3)-O (3)-H (3A)	108 (2)		
		C (5)-O (4)-C (4)	115.82 (11)		
		C (6)-O (5)-H (5A)	109.0 (18)		
		C (5)-O (6)-C (7)	113.72 (11)		
		C (12)-O (7)-H (7A)	105.8 (16)		
		C (7)-O (8)-C (10)	111.69 (11)		
		C (11)-O (9)-H (9A)	108.6 (17)		
		C (9)-O (10)-H (10A)	104.2 (16)		
		C (8)-O (11)-H (11)	110.8 (16)		

UV-visible spectroscopy study: The UV-visible absorption spectrum of sucrose in liquid phase using methanol as a solvent is shown in Fig. 7, recorded in the range of 200-900 nm. The cut off wavelength for this crystal is found to be 253 nm are attributed to the overlapping of π-π* transition. The absorption is very low and found to be steady from 253-900 nm. It is advantageous of the materials for good optical devices.

HOMO-LUMO analysis: The electronic absorption corresponding to the transition from the ground state to the first excited state is mainly described by one electron excitation from the Highest Occupied Molecular Orbital (HOMO) to the Lowest Unoccupied Molecular Orbital (LUMO) (Kavitha *et al*., 2010; Prasad *et al*., 2010). The HOMO represents the ability to donate an electron whereas LUMO represents the ability to obtain an electron. The HOMO locates on the glucofuran ring. The LUMO is located on the glucopyran ring. Consequently, the HOMO-LUMO transition implies an electron density transfer from the orbitals are localized on the rings, both orbitals are π-antibonding-type orbitals.

The frontier molecular orbital's of sucrose is shown in Fig. 8. The energy of HOMO, LUMO and ΔE gap are -6.7152, 1.4536 and-8.1688 eV, respectively.

The calculated Self Consistent Field (SCF) energy of sucrose is-1297.5558 AU at B3LYP/6-311 G(d,p). The HOMO and LUMO energy gap explains the fact that eventual charge transfer interaction is taking place within the molecule.

Molecular Electrostatic Potential (MESP): The Electrostatic Potential (ESP), Electron Density (ED), the Molecular Electrostatic Potential (MESP) and contour map figures of sucrose molecule was calculated and displayed in Fig. 9a-c. The electron density surface can be used to locate atoms, emphasize electron densities associated with chemical bond. The ED plots for sucrose molecule show a uniform distribution. However, it can be seen from the ESP figures, while the negative ESP is localized more over the oxygen over the glucofuran ring and glucopyran ring is reflected as a yellowish blob, the positive ESP is localized on the rest of the molecules. This result is expected, because ESP correlates with electro negativity and partial charges.

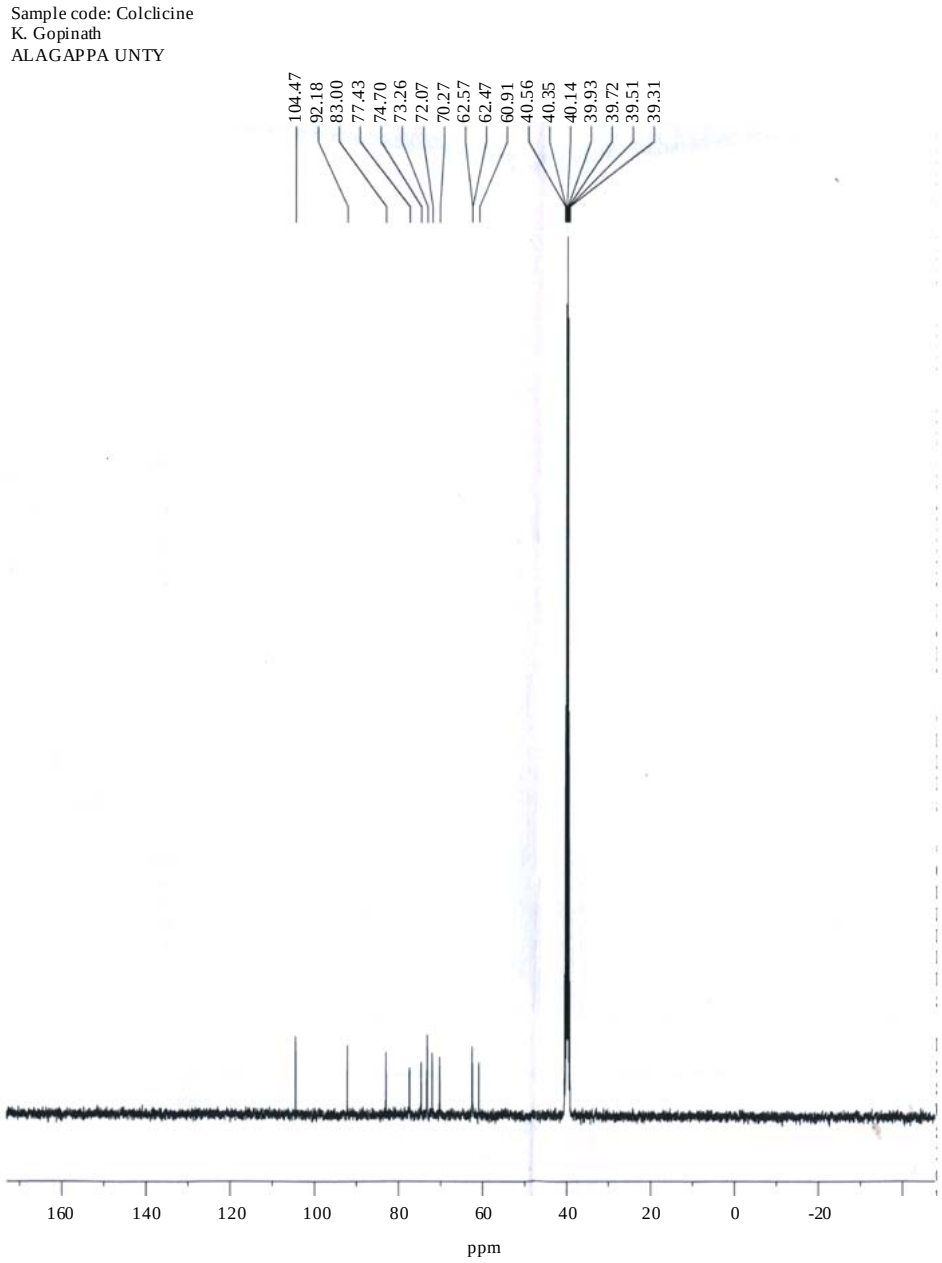

Fig. 5: ^{13}C-NMR analysis of sucrose crystal

The MESP is a plot of electrostatic potential mapped onto the constant electron density surface. The MESP surface super-imposed on top of the total energy density. The MESP is a useful property to study reactivity given that an approaching electrophile will be attracted to negative region (where the electron distribution effect is dominant). In the majority of the MESPs, while the maximum negative region which is preferred site for electrophilic attack indication as red color, the maximum positive region which preferred site for nucleophilic attack symptoms as blue color. The importance of MEP lies in the fact that it is simultaneous displays molecular size, shape as well as positive, negative and neutral electrostatic potential regions in terms of color grading

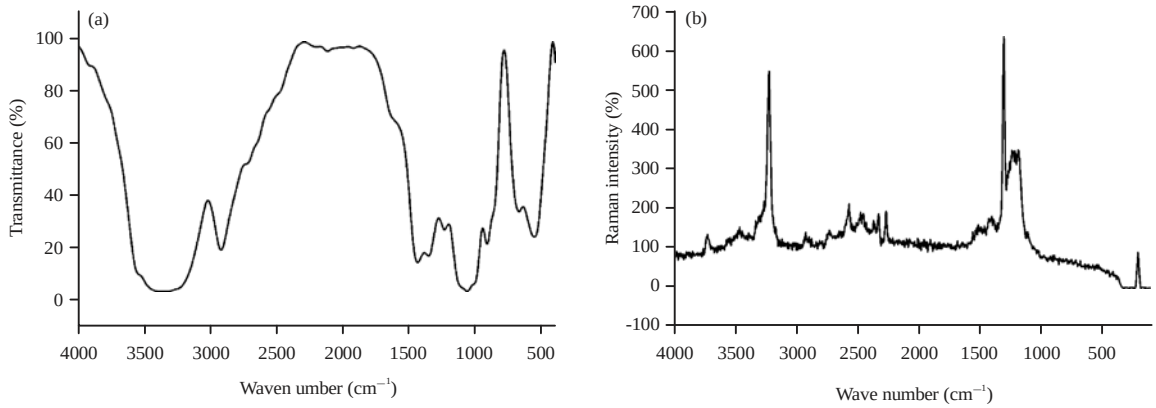

Fig. 6(a-b): (a) FT-IR spectrum and (b) Micro-Raman spectrum of sucrose sample

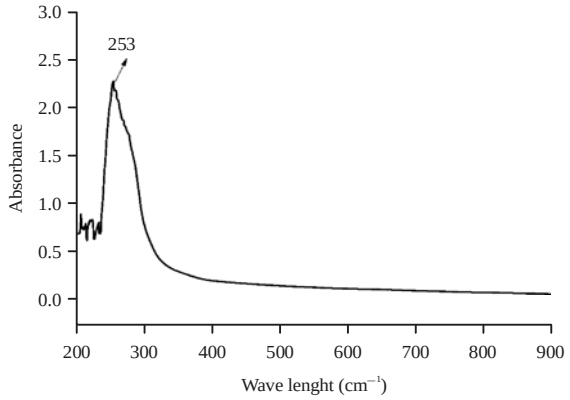

Fig. 7: UV-Vis absorption spectrum of sucrose sample

Table 5: Hydrogen bonding (Å and °)

D-H...A	d(D-H)	d(H...A)	d(D...A)	<(DHA)
O (11)-H (11)...O (10)#1	0.81 (3)	2.06 (3)	2.8675 (19)	170 (2)
O (1)-H (1A)...O (9)#2	0.83 (3)	2.03 (3)	2.8553 (19)	174 (2)
O (10)-H (10A)...O (7)#3	0.84 (2)	1.89 (2)	2.7167 (17)	169 (2)
O (9)-H (9A)...O (4)	0.90 (3)	1.96 (3)	2.8509 (16)	169 (3)
O (7)-H (7A)...O (1)	0.85 (3)	1.97 (3)	2.7809 (18)	158 (2)
O (2)-H (2A)...O (11)#4	0.77 (2)	2.10 (2)	2.8688 (18)	171 (2)
O (3)-H (3A)...O (8)#5	0.76 (3)	2.44 (3)	2.8399 (18)	115 (3)
O (3)-H (3A)...O (2)	0.76 (3)	2.53 (3)	2.880 (2)	110 (3)
O (5)-H (5A)...O (2)#6	0.92 (3)	1.95 (3)	2.848 (2)	164 (3)

Symmetry transformations used to generate equivalent atoms: #1: x,y-1/2,-z+1, #2: x+1,y,z, #3: x-1,y,z, #4: x+1,y-1/2,-z+1, #5: x,y-1,z, #6: x+1,y+1/2,-z+2

(Fig. 9c) and is very useful in research of molecular structure with its physiochemical property relationship (Orozcoa and Luqueb, 1996; Scrocco and Tomasi, 1978). The resulting surface simultaneously displays molecular size and shape and electrostatic potential value.

The different values of the electrostatic potential at the surface are represented by different colors. The potential increases in the order red<orange<yellow<green<blue. The color code of these maps is the range between the-0.0738 AU (Deepest red) to 0.0738 AU (Deepest blue) in sucrose molecules, whereas, blue color indicates the strongest attraction and red color indicates the strongest repulsion. The regions of negative V(r) are usually associated with the lone pair of electro native atoms. As can be seen from the MEP map of the sucrose molecule, while regions having the

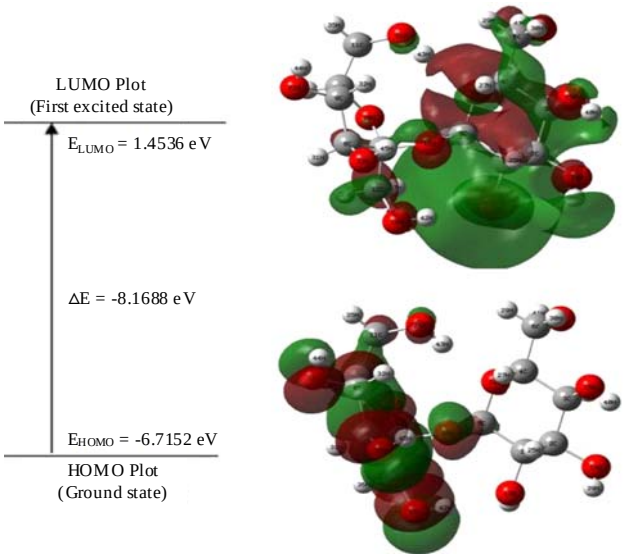

Fig. 8: Atomic orbital compositions of the frontier molecular orbital of sucrose

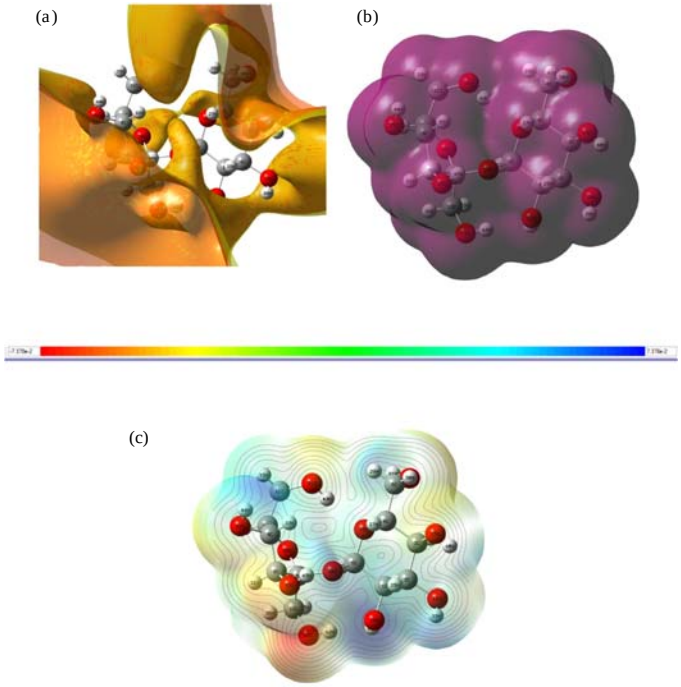

Fig. 9(a-c): (a) Electrostatic potential, (b) Electron density and (c) Molecular electrostatic potential map in gas phase for sucrose molecule

negative potential are over the electronegative atom (oxygen atoms), the regions having the positive potential are over the hydrogen atoms. The contour map of electrostatic potential of the sucrose molecule constructed by the B3LYP/6-311 G(d, p) basis set is shown in Fig. 9c also confirms the different negative and positive potential sites of the molecules in accordance with the total electron density surface.

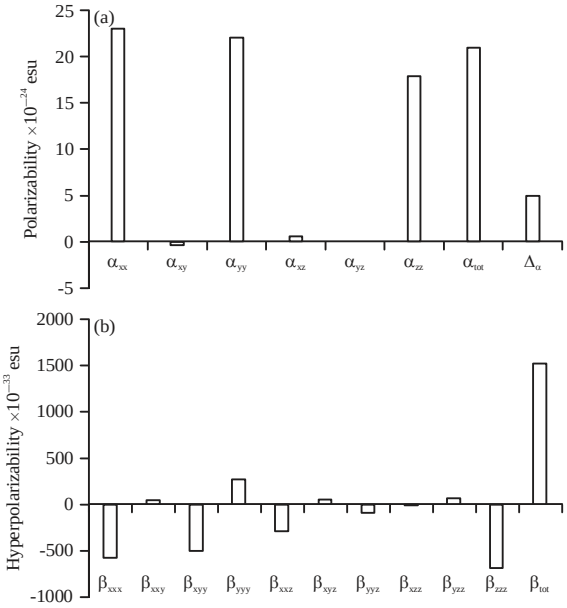

Fig. 10(a-b): (a) Polarizabilty and (b) First order hyperpolarizability B3LYP/6-311 G(d,p) of sucrose molecules

Non-linear optical properties: The mean polarizability (α_{tot}), anisotropy of polarizability (α) and average value of the first order hyperpolarizability (β_{tot}) of sucrose are calculated using B3LYP/6-311 G(d,p) basis set, based on the finite-field approach. In the presence of an applied electric field, the energy of a system is a function of the electric field. First order hyperpolarizalbility is a third rank tensor that can be described by 3×3×3 matrices. The 27 components of the 3D matrix can be reduced to 10 components due to the Kleinman symmetry (Kleinman, 1962). It can be given in the lower tetrahedral format. It is obvious that lower part of the 3×3×3 matrices is a tetrahedral. The components of β are defined as the coefficients in the Taylor series expansion of the energy in the external electric field. When the external electric field is weak and homogeneous, this expansion becomes:

$$E = E^0 - \mu_\alpha F_\alpha - 1/2\alpha_{\alpha\beta} F_\alpha F_\beta - 1/6\, \beta_{\alpha\beta\gamma} F_\alpha F_\beta F_\gamma + \ldots.. \quad (1)$$

where, E^0 is the energy of the unperturbed molecules, F_α in the field at the region, μ_α, $\alpha_{\alpha\beta}$ and $\beta_{\alpha\beta\gamma}$ are the components of dipole moments, polarizability and the first order hyperpolarizability, respectively. The polarizability (α_{xx}, α_{xy}, α_{yy}, α_{xz}, α_{yz}, α_{zz}) and first order hyperpolarizability (β_{xxx}, β_{xxy}, β_{xyy}, β_{yyy}, β_{xxz}, β_{xyz}, β_{yyz}, β_{xzz}, β_{yzz}, β_{zzz}) tensor can be obtained the output file of Gaussian 09 W. However, α and β values of Gaussian output are in Atomic Units (AU) therefore, they have been converted into electronic units (esu) (for α_{tot}, 1 AU = 0.1482×10^{-24} esu and for β_{tot}, 1 AU = 8.6393×10^{-33} esu). The mean polarizability (α_{tot}), anisotropy of polarizability (α) and average value of the first order hyperpolarizability (β_{tot}) can be calculated using the (2)-(4), respectively.

$$\alpha_{tot} = 1/3\, (\alpha_{xx} + \alpha_{yy} + \alpha_{zz}) \quad (2)$$

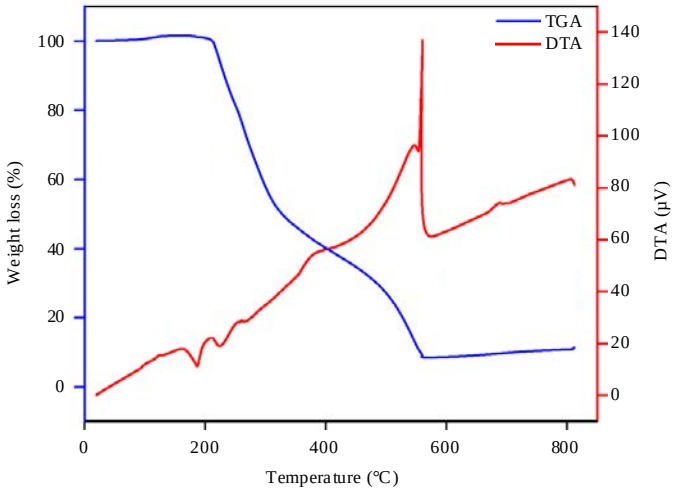

Fig. 11: TG-DTA analysis of sucrose sample

$$\Delta\alpha = \frac{1}{\sqrt{2}}[(\alpha_{xx}-\alpha_{yy})^2+(\alpha_{yy}-\alpha_{zz})^2+(\alpha_{zz}-\alpha_{xx})^2+6\alpha_{xy}^2+6\alpha_{yz}^2]^{1/2} \quad (3)$$

$$\beta_{tot} = [(\beta_{xxx}+\beta_{xyy}+\beta_{xzz})^2+(\beta_{yyy}+\beta_{yzz}+\beta_{yxx})^2+(\beta_{zzz}+\beta_{zxx}+\beta_{zyy})^2]^{½} \quad (4)$$

The calculated parameters as described above are shown in Fig. 10a,b for sucrose crystal. The calculated dipole moment is equal to 2.3544 Debye (D). Total polarizability (α_{tot}) is calculated as 21.1191×10^{-24} esu for sucrose crystal using B3LYP/6-311 G(d, p) basis set. The first order hyperpolarizability is determined by the electron excitations that involve both the ground and excited states. Besides transition energy and transition dipole moment, the dipole moment difference between the ground and excited states is also important in the calculation of β_{tot}. The first order hyperpolarizability values (β_{tot}) of the sucrose crystal are found to be 1533.639×10^{-33} esu. The first order hyperpolarizability β_{tot} dominated by the longitudinal components β_{zzz}. Domination of particular component indicates on a substantial delocalization of charges in the direction.

Thermal studies: Thermo Gravimetric/differential Thermal Analysis (TG/DTA) measurement is used to examine the thermal stability of the crystalline sample. The sucrose sample recorded in the temperature range 30-800°C at a heating rate of 20°C/min in nitrogen atmosphere is shown in Fig. 11. From the TG analysis, the sample exhibits three stages of decomposition taking place at 209, 322 and 558°C, respectively. The TG curve shows that up to 209°C their weight is 100% (no weight loss) for sucrose sample. The sucrose sample shows the major weight loss 48.6648% in the temperature range between 209 to 322°C. This can be attributed to decomposition of –OH groups which are not hydrogen bonded, in addition to expulsion of –CO, H_2 and CO_2. The TG analysis shows the 100% weight loss between 322-558°C. At this stage, there is a degradation leading to the formation of a thermally stable species maintaining stability up to 800°C.

The DT analysis exhibits three endothermic peaks, at around 195, 226 and 400°C, respectively. The form of heat induced decomposition. Since all the decomposition peaks are endothermic, there is no oxidation reaction when the sucrose is subjected to heat changes. Therefore, the three stages of weight loss are shown in TG owing to endothermic peaks.

Table 6: Theoretically computed total energy, zero-point vibrational energy, rotational constant, rotational temperature, vibrational temperature, thermal energy, molar capacity at constant volume and entropy for sucrose crystal

Parameters	B3LYP /6-311 G (d,p)
Zero-point vibrational energy (Kcal/Mol)	243.37578
Rotational constants (GHz)	
A	0.34923
B	0.21848
C	0.16320
Rotational temperature(K)	
A	0.01676
B	0.01049
C	0.00783
Thermal energy (KCal/Mol)	
Total	251.201
Translation	0.889
Rotational	0.889
Vibrational	249.423
Molar capacity at constant volume (Cal/Mol-Kelvin)	
Total	57.312
Translation	2.981
Rotational	2.981
Vibrational	51.351
Entropy (Cal/Mol-Kelvin)	
Total	110.078
Translation	43.384
Rotational	34.511
Vibrational	32.183

Thermodynamic properties: The calculated several thermodynamic parameters have been presented in Table 6. The Zero-Point Vibrational Energies (ZPVE), rotational energy, rotational temperature, thermal energy, molar capacity at constant volume and entropy were calculated by B3LYP/6-311 G(d, p) basis set. The thermodynamic properties are very much useful in the chemical interactions of the sucrose compound.

CONCLUSION

In present investigation, sucrose crystals were grown using the isolated from the hot MeOH extract of the rhizome powder of *G. superba.* The X-ray single crystal structural refinement indicated monoclinic structure and good crystalline quality. Differential thermal analysis and thermal gravimetric analysis clearly showed thermal decomposition of sucrose was considered to start at 186°C. IR and Raman studies on the grown crystals revealed the presence of various -OH, $-CH_2$, etc., groups as the respective vibration frequency peaks were assigned. The UV-visible spectrum confirmed that the crystal was sharp and strong absorbance peak at 253 nm. The stability of sucrose was justified by means of HOMO-LUMO analyses. The theoretical molecular structures of sucrose were determined by the B3LYP/6-311 G(d, p). It is suggested this technique will be used for other tuberous medicinal plants for commercial purpose.

ACKNOWLEDGMENTS

We thank, the Sophisticated Analytical Instrument Facility at the Indian Institute of Technology, Madras for X-ray data collection using the Bruker X8 KAPPA APEX-II CCD diffractometer and also thank to the University Grants Commission (UGC), New Delhi, for providing the fund for major research project (37-14/2009-SR).

REFERENCES

Arumugam, A. and K. Gopinath, 2012. *In vitro* micropropagation using corm bud explants: An endangered medicinal plant of *Gloriosa superba* L. Asian J. Biotechnol., 4: 120-128.

Arumugam, A., C. Karthikeyan, A.S.H. Hameed, K. Gopinath, S. Gowri and V. Karthika, 2015. Synthesis of cerium oxide nanoparticles using *Gloriosa superba* L. leaf extract and their structural, optical and antibacterial properties. Mater. Sci. Eng.: C, 49: 408-415.

Bharathi, P., D. Philomina and S. Chakkaravarthi, 2006. Antimitotic effect of colchicine from six different species of Gloriosa in onion roots (*Allium cepa*). J. Med. Sci., 6: 420-425.

Casado, J., L.L. Miller, K.R. Mann, T.M. Pappenfus and Y. Kanemitsu *et al*., 2002. Combined spectroelectrochemical and theoretical study of a vinylene-bridged sexithiophene cooligomer: Analysis of the π-electron delocalization and of the electronic defects generated upon doping. J. Phys. Chem. B., 106: 3872-3881.

Chitra, R. and K. Rajamani, 2010. Assessment of different glory lily (*Gloriosa superba* L.) accessions for biochemical traits. Res. J. Med. Plant, 4: 21-25.

Gu, H., P. Tian, M. Guo, Y. Li and X. Hao, 2012. Low-temperature electrolytic coloration and spectral properties of sucrose crystals. Spectrochimica Acta Part A: Mol. Biomol. Spectrosc., 91: 269-271.

Hamzaoui, A.H., K. Farah, K. Marzougui, S. Horchani, N.B. Nessib and A. M'Nif, 2009. pH-Metric study of gamma-irradiated table sugar for dosimetry purpose. Radiat. Meas., 44: 374-377.

Hanson, J.C., L.C. Sieker and L.H. Jensen, 1973. Sucrose: X-ray refinement and comparison with neutron refinement. Acta Crystallographica Sect. B: truct. Crystallogr. Cryst. Chem., 29: 797-808.

Hynes, R.C. and Y.L. Page, 1991. Sucrose, a convenient test crystal for absolute structures. J. Applied Crystallogr., 24: 352-354.

Jana, S. and G.S. Shekhawat, 2011. Critical review on medicinally potent plant species: *Gloriosa superba*. Fitoterapia, 82: 293-301.

Jantas, R. and B. Delczyk, 2005. Preparation characterisation and antibacterial properties of sucrose-1-naphtylacetic acid adduct. Fibres Text. Eastern Eur., 13: 60-63.

Kaminskii, A.A., 2003. Stimulated Raman scattering by $C_{12}H_{22}O_{11}$ sugar (sucrose). Crystallogr. Rep., 48: 295-299.

Kavitha, E., N. Sundaraganesan and S. Sebastian, 2010. Molecular structure, vibrational spectroscopic and HOMO, LUMO studies of 4-nitroaniline by density functional method. Indian J. Pure Applied Phys., 48: 20-30.

Kleinman, D.A., 1962. Theory of second harmonic generation of light. Phys. Rev., 128: 1761-1775.

Kraybill, H.R., R.L. Smith and E.D. Walter, 1937. The isolation of sucrose from soybeans. J. Am. Chem. Soc., 59: 2470-2471.

Kumar, C.N., S.K. Jadhav, K.L. Tiwari and Q. Afaque, 2015. *In vitro* tuberization and colchicine content analysis of *Gloriosa superba* L. Biotechnology, 14: 142-147.

Kumaresan, R. and S.M. Babu, 1997. Crystal growth and characterization of sucrose single crystals. Mater. Chem. Phys., 49: 83-86.

Lee, C., W. Yang and R.G. Parr, 1988. Development of the colle-salvetti correlation-energy formula into a functional of the electron density. Phys. Rev. B, 37: 785-789.

Luzardo, M.C., F. Amalfa, A.M. Nunez, S. Diaz, A.C.B. de Lopez and E.A. Disalvo, 2000. Effect of trehalose and sucrose on the hydration and dipole potential of lipid bilayers. Biophys. J., 78: 2452-2458.

Michalska, D., D.C. Bienko, A.J.A. Abkowicz-Bienko and Z. Latajka, 1996. Density functional, hartree-fock and mp2 studies on the vibrational spectrum of phenol. J. Phys. Chem., 100: 17786-17790.

Nakajima, T. and T. Otsuki, 1990. Dosimetry for radiation emergencies: radiation-induced free radicals in sugar of various countries and the effect of pulverizing on the ESR signal. Int. J. Radiat. Applic. Instrum. Part A: Applied Radiat. Isotopes, 41: 359-365.

Naumann, C.P., D. Schultz and D. Helm, 1996. What Can Infrared Spectroscopy Tell us about the Structure and Composition of Intact Bacterial Cell? In: Infrared Spectroscopy of Biomolecules, Mantsch, H.H. and D. Chapman (Eds.). Wiley, New York, USA., ISBN-13: 9780471021841, pp: 279-310.

Orozcoa, M. and F.J. Luqueb, 1996. Generalization of the molecular electrostatic potential for the study of noncovalent interactions. Theoret. Comput. Chem., 3: 181-218.

Peimel-Stuglik, Z., 2010. In search of an ecological dosimeter for high dose measurements: Aqueous sucrose solutions. Applied Radiat. Isot., 68: 654-657.

Ponce-Lee, E.L., A. Olivares-Perez and I. Fuentes-Tapia, 2004. Sugar (sucrose) holograms. Opt. Mater., 26: 5-10.

Prasad, O., L. Sinha and N. Kumar, 2010. Theoretical Raman and IR spectra of tegafur and comparison of molecular electrostatic potential surfaces, polarizability and hyerpolarizability of tegafur with 5-fluoro-uracil by density functional theory. J. Atomic Mol. Sci., 1: 201-214.

Predoi, D., 2010. Physico-chemical studies of sucrose thin films. Digest J. Nnaomater. Biostruct., 5: 373-377.

Ramalakshmi, S., K. Muthuchelian and K. Swaminathan, 2012. Comparative studies on removal of fast green dye from aqueous solutions by activated carbon prepared from *Gloriosa superba* waste and *Alternaria raphani* fungal biomass. J. Environ. Sci. Technol., 5: 222-231.

Ryzhikov, V.D., O.D. Opolonin, S.V. Naidenov, D.N. Kozin, E.K. Lisetskaya and V.L. Danilenko, 2005. Studies of two-energy linear detector matrix for X-ray osteodensitometry. Biomed. Eng., 39: 65-68.

Scrocco, E. and J. Tomasi, 1978. Electronic molecular structure, reactivity and intermolecular forces: An euristic interpretation by means of electrostatic molecular potentials. Adv. Quantum Chem., 11: 115-193.

Son, P.V., T. Fujita and K. Ohshima, 2010. Kinetics of crystalline-noncrystalline phase transition in sucrose. J. Phys. Soc. Jpn., Vol. 79. 10.1143/JPSJ.79.034603

Thamilarasan, V., A. Jayamani, P. Manisankar, Y.I. Kim and N. Sengottuvelan, 2013. Green-emitting phosphorescent iridium(III) complex: Structural, photophysical and electrochemical properties. Inorganica Chimica Acta, 408: 240-245.

Yadava, K., A. Aggarwal and N. Singh, 2013. Evaluation of genetic fidelity among micropropagated plants of *Gloriosa superba* L. using DNA-based markers-a potential medicinal plant. Fitoterapia, 89: 265-270.